JMEPEG (2012) 21:2622–2627
DOI: 10.1007/s11665-012-0392-z

1059-9495/$19.00

Wear Properties of Porous NiTi Orthopedic Shape Memory Alloy

Shuilin Wu, Xiangmei Liu, K.W.K. Yeung, Z.S. Xu, C.Y. Chung, and Paul K. Chu

(Submitted March 10, 2012; in revised form September 7, 2012)

Porous NiTi shape memory alloy (SMA) scaffolds have great potential to be used as orthopedic implants because of their porous structure and superior physical properties. Its metallic nature provides it with better mechanical properties and Young's modulus close to that of natural bones. Besides allowing tissue ingrowth and transfer of nutrients, porous SMA possesses unique pseudoelastic properties compatible to natural hard tissues like bones and tendons, thus expediting in vivo osseointegration. However, the nickel release from debris and the metal surface may cause osteocytic osteolysis at the interface between the artificial implants and bone tissues. Subsequent mobilization may finally lead to implant failure. In this study, the wear properties of porous NiTi with different porosities processed at different treatment temperatures are determined. The results of the study show that the porosity, phase transformation temperature, and annealing temperature are major factors influencing the wear characteristics of porous NiTi SMA.

Keywords NiTi, orthopedic implants, porosity, scaffold, wear resistance

1. Introduction

Owing to the deficiency of autogenous grafts and possible rejection of allografts, it is imperative to develop synthetic bone grafts that can satisfy the increasing market demand (Ref 1). As one of the most promising man-made bone grafts, porous nickel-titanium (NiTi) shape memory alloy (SMA) allows ingrowth of osteoblasts and tissues, thus favoring long-term fixation of bone implants (Ref 2-4). Besides the good mechanical properties inherent from its metallic nature, porous NiTi has lower Young's modulus close to that human bone and pseudoelastic biomechanical behaviors similar to hard tissues like bone and tendon (Ref 2, 5, 6). However, some practical problems still need to be solved before clinical application. For example, release of nickel into surrounding tissues and corrosion of NiTi may induce cytotoxicity (Ref 7, 8). Some surface modification techniques have been developed to obtain enhanced biocompatibility (Ref 9-13). Clinically, movement or mobilization of metal-implants is one of the main failure mechanisms. The wear debris shed from implants at the interface with biological tissues can often lead to massive osteolysis, subsequent mobilization of implants, and finally, catastrophic failure (Ref 14, 15). Hence, it is important to understand the tribological behavior of SMA implants during the design stage.

In the last decade, the tribological performance of dense NiTi SMAs has been widely investigated (Ref 16-21). In comparison with traditional metals, dense NiTi SMAs possess much better wear resistance, which is ascribed to their unique pseudoelasticity (Ref 22), lower E/H of TiNi (Ref 20), and combined effects of the smaller Young's modulus and small transformation stress (Ref 21). However, previous studies have primarily focused on dense materials and the corresponding pseudoelasticity. In this study, the tribological behavior of porous NiTi SMAs is evaluated.

2. Experimental Procedures

The porous NiTi samples were prepared by a novel powder metallurgical (PM) method, namely, capsule-free hot isostatic pressing (CF-HIP). Equiatomic titanium and nickel powders from Shanghai Reagent Corporation were used as the starting materials. They were thoroughly mixed in a horizontal universal ball mill together with the foaming agent, ammonium acid carbonate (NH_4HCO_3) powders, and then pressed into green compacts under a cold pressure of 200 MPa. Before sintering at 150 MPa and 1050 °C, a preheating process at 200 °C was performed to remove the foaming agent. The sintering process was carried out in a HIP unit under argon. By

This article is an invited paper selected from presentations at the International Conference on Shape Memory and Superelastic Technologies 2011, held November 6-9, 2011, in Hong Kong, China, and has been expanded from the original presentation.

Shuilin Wu, Ministry-of-Education Key Laboratory for the Green Preparation and Application of Functional Materials, School of Materials Science and Engineering, Hubei University, Wuhan 430062, People's Republic of China and Department of Physics & Materials Science, City University of Hong Kong, Tat Chee Avenue, Kowloon, Hong Kong, People's Republic of China; **Xiangmei Liu** and **Z.S. Xu**, Ministry-of-Education Key Laboratory for the Green Preparation and Application of Functional Materials, School of Materials Science and Engineering, Hubei University, Wuhan 430062, People's Republic of China; **K.W.K. Yeung**, Division of Spine Surgery, Department of Orthopaedics and Traumatology, The University of Hong Kong, Pokfulam, Hong Kong, People's Republic of China; and **C.Y. Chung** and **Paul K. Chu**, Department of Physics & Materials Science, City University of Hong Kong, Tat Chee Avenue, Kowloon, Hong Kong, People's Republic of China. Contact e-mails: shuilin.wu@gmail.com and paul.chu@cityu.edu.hk.

adjusting the amount of the foaming agent, porous samples with porosities of 18 and 36% were obtained and designated as L (low) and H (high), respectively. More details about the CF-HIP process can be found in previous publications (Ref 23, 24). 2-mm-thick samples with a diameter of 12.7 mm were mechanically ground by SiC sandpaper progressively up to 800 grit, ultrasonically rinsed with acetone and ethanol, and then oven-dried before further experiments.

The wear test was performed on flat porous NiTi samples at room temperature in atmosphere using a ball-on-disk wear tester. The balls used in the abrasive wear tests were standard WC-Co ones with a diameter of 5 mm. A circular wear track was created on the sample by offsetting the ball relative to the center of rotation of the sample. Under an applied load of 2 N, the balls scribed a 5-mm-diameter wear trace on the sample surface as it rotated at a speed 200 RPM. The surface wear morphology was examined by scanning electron microscopy (SEM JSM5200 and JSM 820). The chemical composition of the wear debris was determined by energy-dispersive x-ray spectroscopy (EDS). The hardness of the porous NiTi was measured by nanoindentation to a depth of 2000 nm (MTS Nano Instruments XP). Differential scanning calorimetry (DSC) thermal analysis was conducted to determine the transformation behavior in the range of −50 to 100 °C.

3. Results and Discussion

Figure 1 shows the tribological performance of the porous NiTi annealed at different temperature under a load of 2 N. Figure 1(a) and (c) shows that the higher porosity sample H has lower friction coefficient and better wear resistance than sample L after 200 and 500 °C annealing. Under dry wearing conditions, the friction coefficients are calculated by the following equation (Ref 25):

$$f = \frac{SA}{W} \quad \text{(Eq 1)}$$

where S is the shearing stress, W is the nominal load, and A is the apparent contact area. Because a porous structure reduces the contact area, a higher porosity induces a smaller contact area consequently yielding smaller friction coefficients.

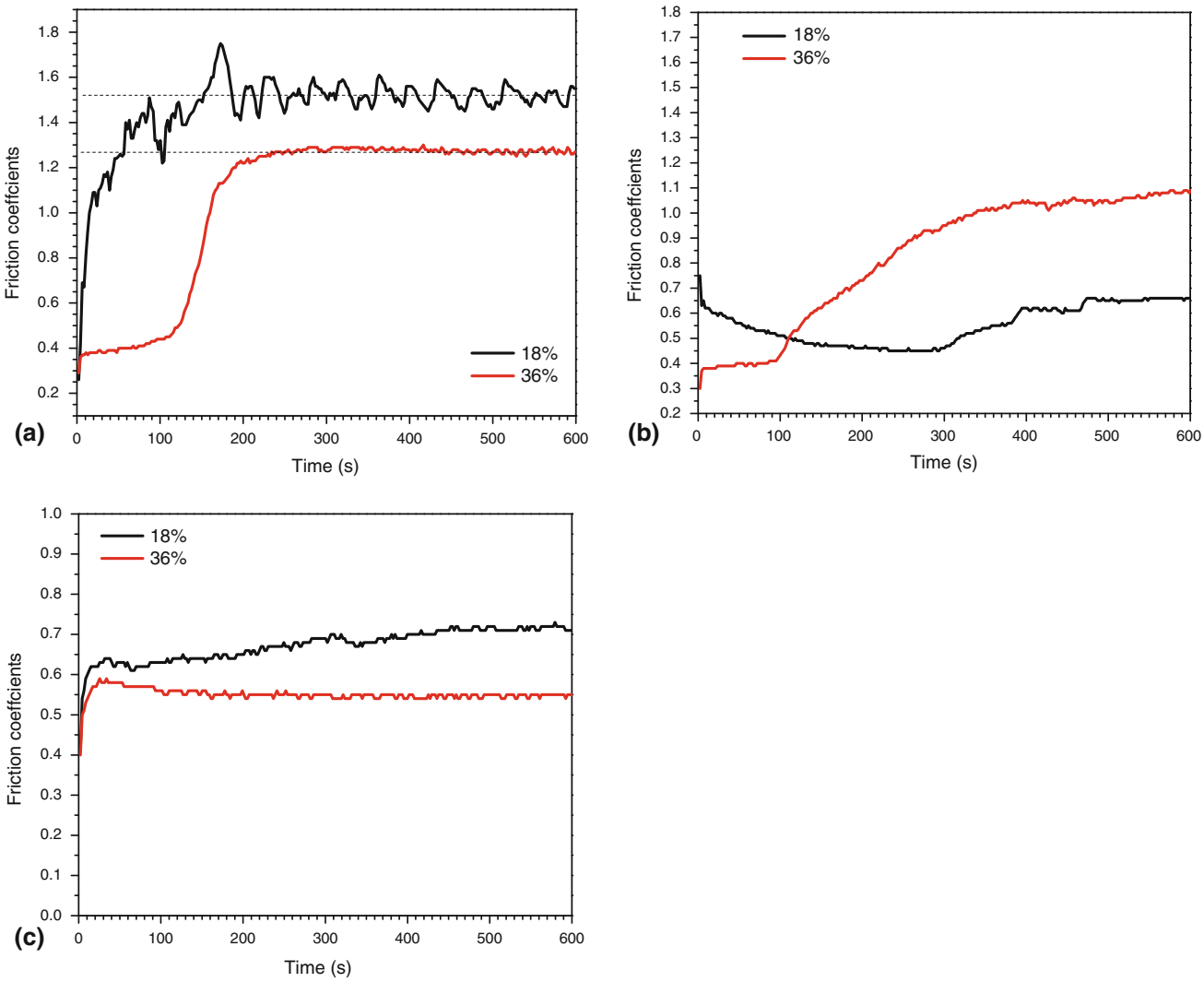

Fig. 1 Evolution of friction coefficients with sliding time on the porous NiTi annealed at different temperatures under a load of 2 N: (a) 200 °C, (b) 400 °C, and (c) 500 °C; % indicates porosity

However, an unexpected phenomenon is observed in the 400 °C annealed porous NiTi sample as shown in Fig. 1(b). Sample L shows lower friction coefficients relative to sample H. Hence, besides porosity, some other factors may also contribute to the tribological behavior. The wear behavior of NiTi may also be affected by its phase constituents (Ref 22) and the martensitic transformation temperature (*Ms*). As shown in Fig. 2(a), sample L is composed of the predominant austenite (B2) phase as well as some minor R-phase (an intermediate rhombohedral distortion of the cubic austenite phase) and B19′ (martensite) phase at room temperature whereas the R-phase is the main phase in sample H (shown in Fig. 2b) as confirmed by XRD reported in our previous articles (Ref 23, 26, 27). As B2 is the harder phase in NiTi SMAs, the hardness of sample L is higher than that of sample H. The hardness measured by nanoindentation also confirms it. The former has an average hardness of about 5.5 GPa and that of the latter is about 3.3 GPa at the depth of 2000 nm. In this case, *Ms* plays a predominant role in the tribological performance of porous NiTi.

Besides the porosity relationship expressed by Eq 1, the pseudoelasticity caused by thermally induced or stress-induced martensitic transformation should have influenced the wear resistance of porous NiTi SMAs substantially. As shown in Fig. 2(b), the 500 °C annealed sample H has an *Ms* temperature of 4.3 °C and peak temperature of −7.4 °C, while the corresponding values are about 24.3 and −18.8 °C for the 500 °C annealed sample L, respectively (Fig. 2a). The results reveal that the phase transformation in sample L is more rapid than that in sample H as the temperature is decreased. It indicates that martensitic transformation in sample L is relatively more difficult compared to that in the latter, because a larger driving force is required to complete the transformation. Consequently, porous sample H exhibits better pseudoelasticity than sample L and it was also be confirmed by our compression tests in our previous report (Ref 23). This is also the factor giving rise to the lower friction coefficient of sample H shown in Fig. 1(c).

Figure 3 shows the evolution of friction coefficients of the porous NiTi annealed at different temperatures under a load of

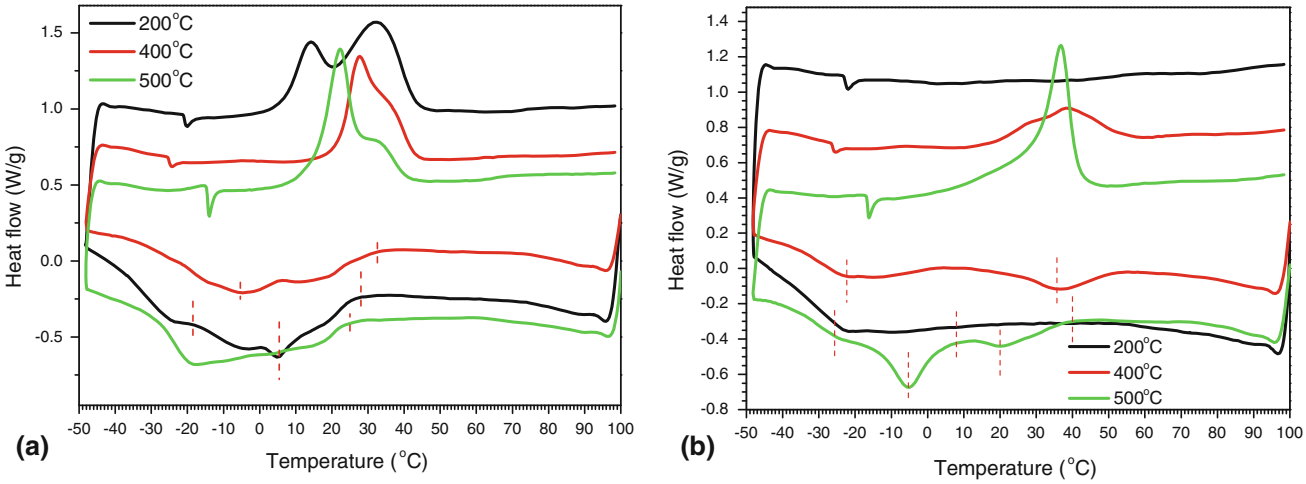

Fig. 2 Phase transformation behavior of porous NiTi annealed at different temperature for 0.5 h: (a) 18% porosity and (b) 36% porosity

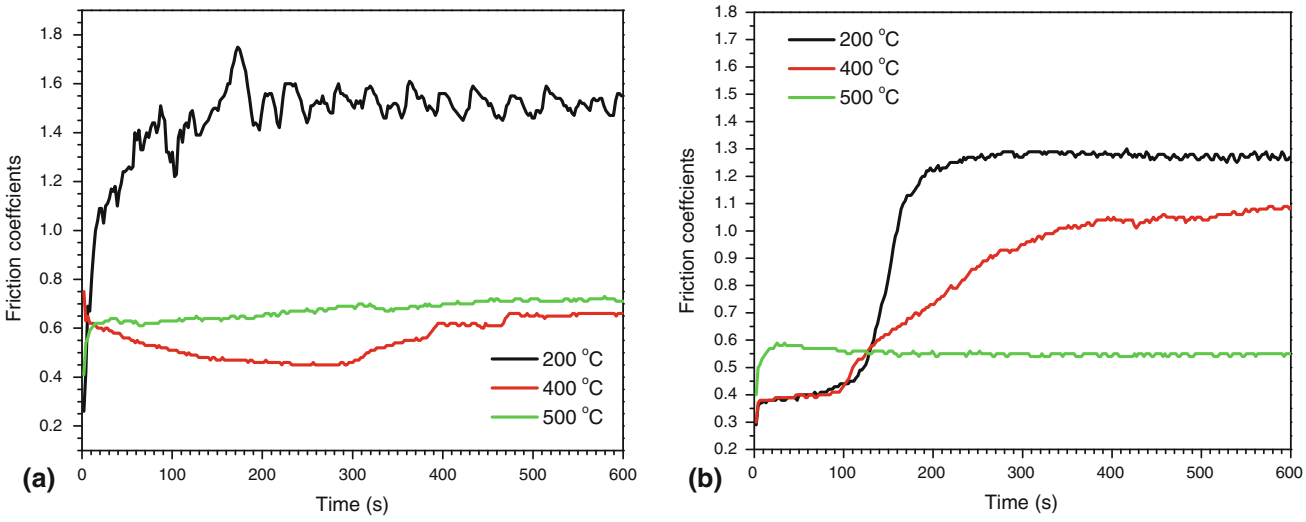

Fig. 3 Evolution of friction coefficients of porous NiTi annealed at 200, 400, and 500 °C under a load of 2 N: (a) 18% porosity and (b) 36% porosity

2 N. As the annealing temperature is increased, the friction coefficients of porous NiTi decrease. The only exception is the 400 °C annealed sample which shows lower friction than the 500 °C one for porous sample L shown in Fig. 3(a). This phenomenon can be explained by the phase transformation behavior during the exothermic process. As shown in Fig. 2(a), although 500 °C annealing induces the lowest *Ms* temperature of 24.3 °C for sample L, 400 °C annealing leads to a peak temperature of −4 °C that is much higher than that of the former, indicating that the phase transformations in the latter proceed more easily than that in the former. Hence, 400 °C annealing yields better pseudoelasticity in sample L, and consequently higher wear resistance. According to Fig. 2(a), although 200 °C annealing can produce the best pseudoelasticity, the lowest hardness is obtained in sample L. Based on nanoindentation, the average hardness values of the 200, 400, and 500 °C annealed sample L are 4.98, 5.71, and 7.3 GPa, respectively. Therefore, sample L shows the worst wear resistance after annealing at 200 °C because it is softer.

In the higher porosity sample H, as shown in Fig. 3(b), the highest annealing temperature of 500 °C yields the lowest friction coefficient because sample H exhibits the best pseudoelasticity according to the DSC curve shown in Fig. 2(b). In addition, at room temperature, the 500 °C annealed sample H is composed of the hard phase B2 and soft phase R whereas the R-phase is the main constituent in the 400 °C annealed sample H. Therefore, the former has higher hardness than the latter. Nanoindentation shows that the average hardness values of sample H after annealing at 200, 400 and 500 °C are 4.73, 3.22, and 4.32 GPa, respectively. Although 200 °C annealing induces the highest harness in sample H, it does not have any pseudoelastic behavior because 200 °C cannot induce the phase transformation (Fig. 2b). Therefore, it has the highest friction coefficient as shown in Fig. 3(b). The presence of the R-phase and the corresponding pseudoelastic properties can lower the friction coefficient.

Figure 4 shows the morphology of the wear tracks on the porous NiTi annealed at 200 °C under a load of 2 N. There is a wide and clear track on the low porosity sample L (Fig. 4a) and the EDS pattern reveals traces of W and Co in the debris (marked by green frame in Fig. 4a) formed during the sliding process (Fig. 4b). In comparison with sample L, high porosity sample H shows a dim track marked by the red arrow in Fig. 4(c). The observation is in good agreement with the deduction of friction coefficient in Fig. 1(a). Figure 5(a) shows a narrow and blurry track (indicated by red arrow) on the surface of the 400 °C annealed sample L under a load of 2 N. The track becomes wider on the 400 °C annealed sample H (marked by red arrows in Fig. 5b), and it is also in accordance with the analysis of friction coefficients in Fig. 1(b). Figure 6(a), reveals a dim track on the surface of the 500 °C annealed sample L under a load of 2 N (marked by red arrow), but no track can be found from the worn surface on the 500 °C annealed sample H under a load of 2 N (Fig. 6b), revealing that the latter has better wear resistance. The wear morphology also supports the aforementioned results of the friction coefficients in Fig. 1(c).

4. Conclusion

The wear resistance of porous NiTi SMAs is investigated. A higher porosity gives better wear resistance. Besides porosity, other factors like the pseudoelastic behavior, phase transformation temperatures, hardness, and phase constituent of the alloys determine the overall tribological performance of the porous NiTi alloy. Similar to other materials, harder phase will result in better wear resistance. A higher annealing temperature typically gives rise to better pseudoelasticity and phases of higher hardness in the higher porosity samples. Weaker pseudoelasticity is observed from the lower porosity samples with higher annealing temperatures. However, the presence of R-phase is also influential in lowering the friction coefficient attributed to its pseudoelastic properties. Altogether, the wear resistance of porous NiTi is determined by the

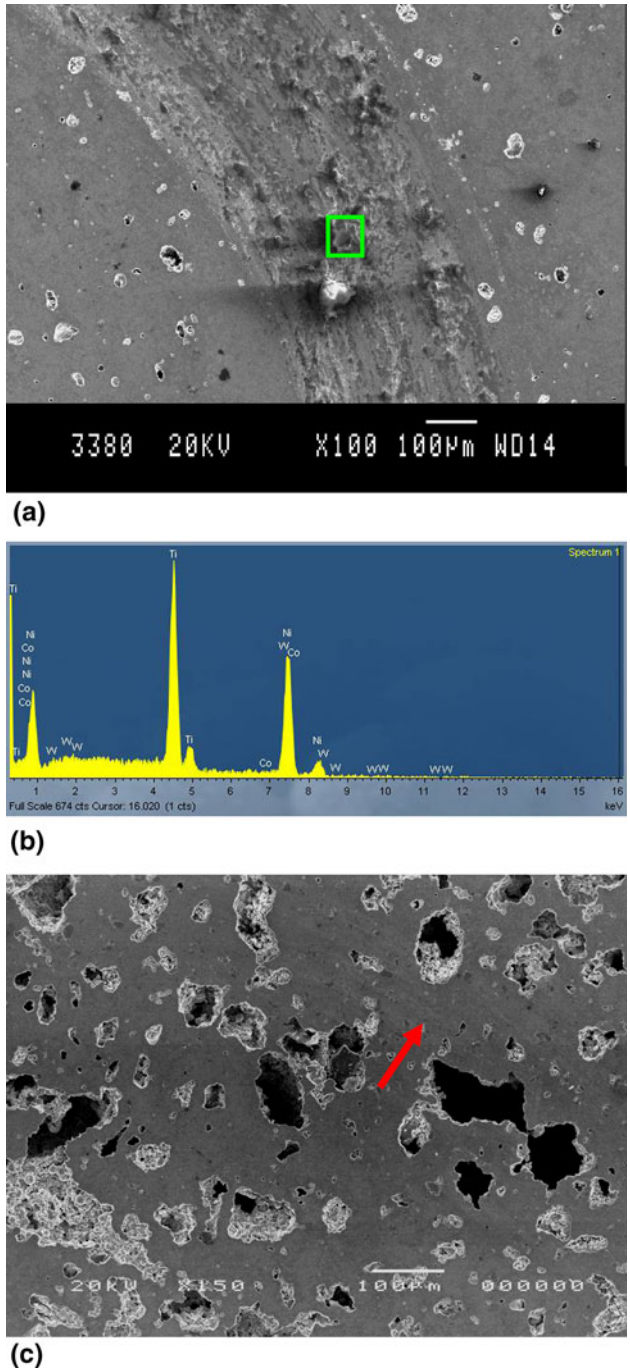

Fig. 4 SEM images of track morphologies of 200 °C annealed porous NiTi under a load of 2 N: (a) 18% porosity, (b) EDS pattern of area indicated by green frame in (a), (c) 36% porosity (Color figure online)

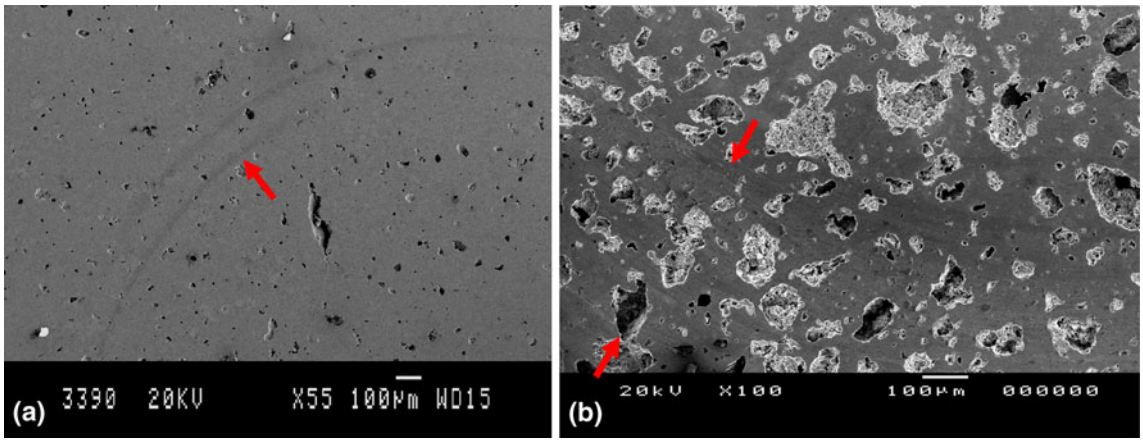

Fig. 5 SEM images showing the track morphology on the 400 °C annealed porous NiTi under a load of 2 N: (a) 18% porosity and (b) 36% porosity

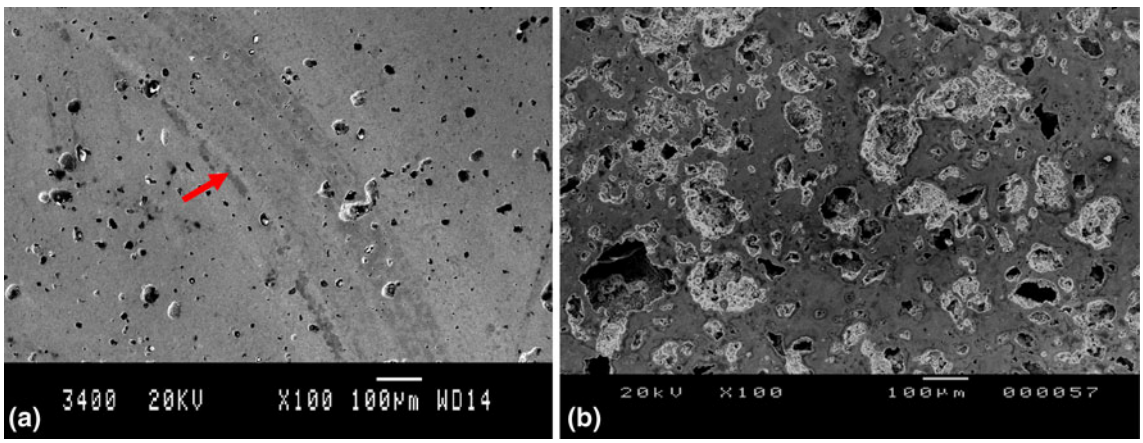

Fig. 6 SEM images of the track morphology of the 500 °C annealed porous NiTi under a load of 2 N: (a) 18% porosity and (b) 36% porosity

combined effects of porosity, pseudoelasticity, and phase constituents. By controlling the amount of the pseudoelastic phase, softer materials may have higher wear resistance relative to the harder materials by varying the friction coefficient.

Acknowledgments

This study is jointly supported by the City University of Hong Kong Applied Research Grant (ARG) No. 9667038, CityU SRG Grant 7002691, the National Natural Science Foundation of China No. 50901032, 51101053, Ministry of Education Specialized Research Foundation for Doctoral Program of Universities No. 20094208120003, the Hubei Provincial Middle-Young Research Fund, Grant No. Q20101010, and the Wuhan ChenGuang Research Program, Grant no. 201150431134.

References

1. R.O. Darouiche, Current Concepts—Treatment of Infections Associated with Surgical Implants, *N. Engl. J. Med.*, 2004, **350**, p 1422–1429
2. X.M. Liu, S.L. Wu, K.W.K. Yeung et al., Relationship Between Osseointegration and Pseudoelastic Biomechanics in Porous NiTi Scaffolds, *Biomaterials*, 2011, **32**, p 330–338
3. A. Bansiddhi, T.D. Sargeant, S.I. Stupp, and D.C. Dunand, Porous NiTi for Bone Implants: A Review, *Acta Biomater.*, 2008, **4**, p 773–782
4. M. Assad, P. Jarzem, M.A. Leroux et al., Porous Titanium-Nickel for Intervertebral Fusion in a Sheep Model: Part 1. Histomorphometric and Radiological Analysis, *J. Biomed. Mater. Res. B*, 2003, **64**, p 107–120
5. N.B. Morgan, Medical Shape Memory Alloy Applications—The Market and Its Products, *Mater. Sci. Eng. A*, 2004, **378**, p 16–23
6. C.H. Turner, Biomechanics of Bone: Determinants of Skeletal Fragility and Bone Quality, *Osteoporos. Int.*, 2002, **13**, p 97–104
7. C.C. Shih, S.J. Lin, Y.L. Chen et al., The Cytotoxicity of Corrosion Products of Nitinol Stent Wire on Cultured Smooth Muscle Cells, *J. Biomed. Mater. Res.*, 2000, **52**, p 395–403
8. J.P. Thyssen, J.D. Johansen, B.C. Carlsen, and T. Menne, Prevalence of Nickel and Cobalt Allergy Among Female Patients with Dermatitis Before and After Danish Government Regulation: A 23-Year Retrospective Study, *J. Am. Acad. Dermatol.*, 2009, **61**, p 799–805
9. S.L. Wu, X.M. Liu, T. Hu et al., A Biomimetic Hierarchical Scaffold: Natural Growth of Nanotitanates on Three-Dimensional Microporous Ti-Based Metals, *Nano Lett.*, 2008, **8**, p 3803–3808
10. C. Pulletikurthi, N. Munroe, P. Gill, S. Pandya, D. Persaud, W. Haider, K. Iyer, and A. McGoron, Cytotoxicity of Ni from Surface-Treated Porous Nitinol (PNT) on Osteoblast Cells, *J. Mater. Eng. Perform.*, 2011, **20**, p 824–829
11. X.M. Liu, S.L. Wu, Y.L. Chan, P.K. Chu, C.Y. Chung, C.L. Chu et al., Surface Characteristics, Biocompatibility and Mechanical Properties of Nickel-Titanium Plasma-Implanted with Nitrogen at Different Implantation Voltages, *J. Biomed. Mater. Res. A*, 2007, **82**, p 469–478
12. S.L. Wu, X.M. Liu, Y.L. Chan, P.K. Chu, C.Y. Chung, C.L. Chu et al., Nickel Release Behavior and Surface Characteristics of Porous NiTi

Shape Memory Alloy Modified by Different Chemical Processes, *J. Biomed. Mater. Res. A*, 2009, **89**, p 483–489

13. E.N. de Camargo, A.O. Lobo, M.M. da Silva et al., Determination of Ni Release in NiTi SMA with Surface Modification by Nitrogen Plasma Immersion Ion Implantation, *J. Mater. Eng. Perform.*, 2011, **20**, p 798–801
14. C.H. Lohmann, Z. Schwartz, G. Koster et al., Phagocytosis of Wear Debris by Osteoblasts Affects Differentiation and Local Factor Production in a Manner Dependent on Particle Composition, *Biomaterials*, 2000, **21**, p 551–561
15. H.C. Amstutz, P. Campbell, N. Kossovsky, and I.C. Clarke, Mechanism and Clinical-Significance of Wear Debris-Induced Osteolysis, *Clin. Orthop. Relat. Res.*, 1992, **276**, p 7–18
16. R. Liu and D.Y. Li, Experimental Studies on Tribological Properties of Pseudoelastic TiNi Alloy with Comparison to Stainless Steel 304, *Metall. Mater. Trans. A*, 2000, **31**, p 2773–2783
17. X.M. Liu, S.L. Wu, Y.L. Chan, P.K. Chu, C.Y. Chung, C.L. Chu et al., Structure and Wear Properties of NiTi Modified by Nitrogen Plasma Immersion Ion Implantation, *Mater. Sci. Eng. A*, 2007, **444**, p 192–197
18. H.Z. Ye, D.Y. Li, and R.L. Eadie, Influences of Porosity on Mechanical and Wear Performance of Pseudoelastic TiNi-Matrix Composites, *J. Mater. Eng. Perform.*, 2001, **10**, p 178–185
19. H.C. Man, S. Zhang, and F.T. Cheng, Improving the Wear Resistance of AA 6061 by Laser Surface Alloying with NiTi, *Mater. Lett.*, 2007, **61**, p 4058–4061
20. C. Zhang and Z.N. Farhat, Sliding Wear of Superelastic TiNi Alloy, *Wear*, 2009, **267**, p 394–400
21. W.Y. Yan, Theoretical Investigation of Wear-Resistance Mechanism of Superelastic Shape Memory Alloy NiTi, *Mater. Sci. Eng. A*, 2006, **427**, p 348–355
22. Y.N. Liang, S.Z. Li, Y.B. Jin, W. Jin, and S. Li, Wear Behavior of a TiNi Alloy, *Wear*, 1996, **198**, p 236–241
23. S.L. Wu, C.Y. Chung, X.M. Liu, P.K. Chu, J.P.Y. Ho, C.L. Chu et al., Pore Formation Mechanism and Characterization of Porous NiTi Shape Memory Alloys Synthesized by Capsule-Free Hot Isostatic Pressing, *Acta Mater.*, 2007, **55**, p 3437–3451
24. S.L. Wu, X.M. Liu, K.W.K. Yeung, T. Hu, Z.S. Xu, C.Y. Chung et al., Hydrogen Release from Titanium Hydride in Foaming of Orthopedic NiTi Scaffolds, *Acta Biomater.*, 2011, **7**, p 1387–1397
25. P. La, Q. Xue, and W. Liu, Effects of Boron Doping on Tribological Properties of Ni3Al-Cr7C3 Coatings Under Dry Sliding, *Wear*, 2001, **249**, p 93–99
26. S.L. Wu, X.M. Liu, P.K. Chu, C.Y. Chung, C.L. Chu, and K.W.K. Yeung, Phase Transformation Behavior of Porous NiTi Alloys Fabricated by Capsule-Free Hot Isostatic Pressing, *J. Alloy. Compd.*, 2008, **449**, p 139–143
27. S.L. Wu, P.K. Chu, X.M. Liu, C.Y. Chung, J.P.Y. Ho, C.L. Chu et al., Surface Characteristics, Mechanical Properties, Cytocompatibility of Oxygen Plasma-Implanted Porous Nickel Titanium Shape Memory Alloy, *J. Biomed. Mater. Res. A*, 2006, **79**, p 139–146